See discussions, stats, and author profiles for this publication at: https://www.researchgate.net/publication/251237923

# Periodically Grafted Amphiphilic Copolymers: Nonionic Analogues of Ionenes

**DATASET** in MACROMOLECULES · MARCH 2012

Impact Factor: 5.8 · DOI: 10.1021/ma2023414

**CITATIONS** 

9

**READS** 

68

## 3 AUTHORS:



## Raj Kumar Roy

Nagoya University

10 PUBLICATIONS 74 CITATIONS

SEE PROFILE



## Bhoje Gowd

National Institute for Interdisciplinary Science...

38 PUBLICATIONS 592 CITATIONS

SEE PROFILE



## Suchitra Ramakrishnan

Eastern Michigan University

**61** PUBLICATIONS **1,322** CITATIONS

SEE PROFILE

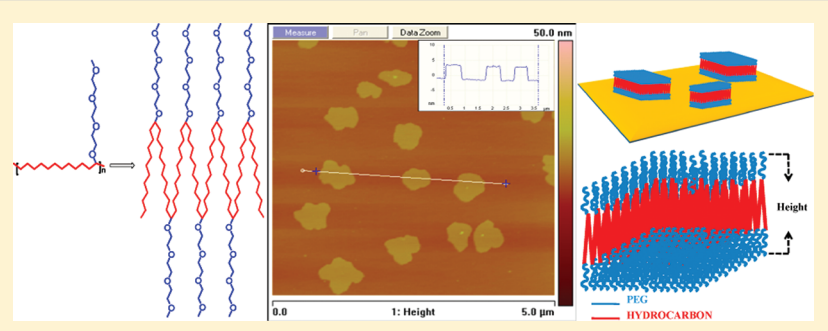


## Periodically Grafted Amphiphilic Copolymers: Nonionic Analogues of Ionenes

Raj Kumar Roy, E. Bhoje Gowd, † and S. Ramakrishnan\*

Department of Inorganic and Physical Chemistry, Indian Institute of Science, Bangalore 560012, India

Supporting Information



ABSTRACT: We describe a novel class of periodically grafted amphiphilic copolymers (PGACs) that could serve as nonionic functional mimics of ionenes, the primary difference being that the periodically occurring charged units along the backbone of ionenes are replaced by hydrophilic oligoethylene glycol segments. The synthesis and properties of this new class of segmented polymers that carry a hydrophobic alkylene polyester backone with periodically placed hydrophilic oligo(oxyethylene) pendant units are presented. When the length of the intervening alkylene segment is adequately long, 22-carbons in this case, and the pendant unit is a hexaethylene glycol monomethyl ether (HEG) segment, the polymer chain appears to adopt a folded zigzag conformation, reminiscent of the accordion-type structure formed by cationic ionenes. This transformation is driven by the intrinsic immiscibility of the alkylene and HEG segments and is reinforced by the strong tendency for long chain alkylene segments to crystallize in a paraffinic lattice. Evidence of the formation of such structures comes from the AFM images, which reveal the formation of remarkably flat pancake-like aggregates that are formed by the lateral aggregation of individually collapsed polymer chains; importantly, the heights of these structures match well with the lamellar layer-spacing obtained from SAXS studies of bulk samples. DSC studies further confirm the crystallization of the intervening alkylene segments, especially when they are long (C22), suggesting the formation of the folded zigzag structures. In a suitably designed PGAC that carries diacetylene units symmetrically placed within the alkylene segment, attempts were made to cross-polymerize the diacetylene units and generate PEGylated nanoparticles. However, these attempts were unsuccessful demonstrating the very stringent geometric requirements for the topotactic polymerization of diacetylenes.

## **■ INTRODUCTION**

It has been known for several decades, since the early work by Rembaum and coworkers, that cationic ionenes wherein the charges reside directly on the polymer backbone with a regular periodicity exhibit a strong tendency to adopt an accordiontype conformation (Scheme 1) when dissolved in water; this is especially true when the number of intervening carbon atoms are large (>12).3 Recently, in an effort to reinforce the collapsed zigzag structures, we prepared cationic ionenes wherein alternate alkylene segments carried electron-rich and electron-deficient aromatic units; this, in addition to reinforcing the formation of folded structures in water due to chargetransfer interactions between the donor and acceptor units, also provided a useful spectroscopic tool to follow the folding process.4

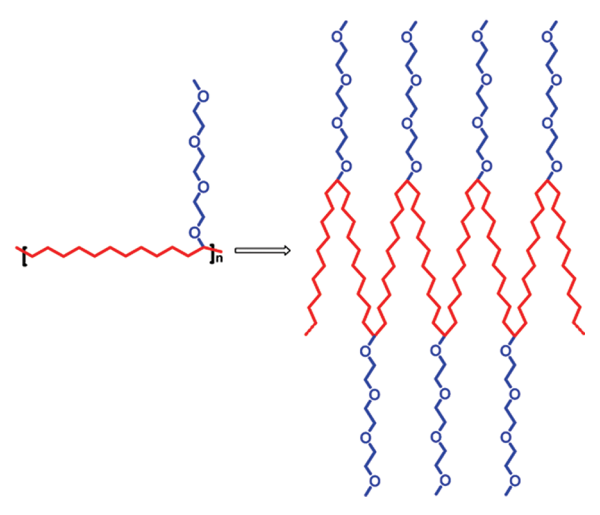
Just as ionenes may be viewed as polymeric (head-to-tail linked) analogues of ionic surfactants, one can also conceptualize a similar polymeric analogue of nonionic surfactants - these would be polymers wherein hydrophilic oligoethylene glycol segments are periodically placed as pendant groups along a linear hydrophobic polymer backbone, as depicted in Scheme 1. Such periodically grafted amphiphilic copolymers (PGACs) could be viewed as nonionic analogues of ionenes and could also be termed nonionic ionenes; as this would help one draw a parallel between the functional similarities that exist between ionic and nonionic surfactants and bring it into the context of their polymeric analogues. As in the case of ionenes, these nonionic analogues may also be expected to form zigzag folded structures (Scheme 1) when the lengths of the alkylene and oxyethylene segments are suitably balanced. In a recent report, Wagener and coworkers described the synthesis of structurally similar systems wherein a long-chain  $\alpha,\omega$ -diene, carrying a

October 19, 2011 Received: Revised: March 13, 2012 Published: March 26, 2012

Scheme 1. Schematic Depiction of the Structures and Collapsed Conformations of Ionenes and Their Nonionic Analogues<sup>a</sup>

## Simple ionenes

## Nonionic analogues



"For simplicity and conceptual clarity, the PEG chains have been shown to adopt an all-trans conformation, which in reality would not be the case.

pendant tri- or tetra-ethylene glycol monomethyl ether segment, was polymerized using ADMET to yield periodically grafted copolymers; however, the focus of their investigations was limited to the study of their solid-state properties, in particular, to examine the influence of the lateral substituent on the crystalline morphology of the alkylene segment using WAXS measurements.

In this report, we describe a simple design and synthesis of two novel kinds of PGACs wherein pendant hexaethylene glycol monomethyl ether (HEG) units are periodically placed along a hydrophobic backbone; the nature and length of the hydrophobic alkylene backbone was varied, and in one case a diacetylene unit was incorporated within the alkylene segment to explore the possibility of photoinduced cross-polymerization of the collapsed zigzag structures.

#### RESULTS AND DISCUSSION

To develop a simple strategy for the synthesis of periodically grafted amphiphilic copolymers (PGACs), we utilized a readily available starting material, such as diethyl malonate; base-catalyzed alkylation of the malonate with hexaethylene glycol monomethyl ether monotosylate<sup>6</sup> yielded the required diester monomer (A) carrying the pendant HEG segment (Scheme 2). The proton NMR spectrum of the monomer was in accordance with the expected structure (Figure 1); interestingly, the

Scheme 2. Structure and Synthesis of Monomers and PGACs

Monomer synthesis

Polymerization

Eto OEt + HO OH DBTL

150 °C

5 Torr

A PGAC-C12

Other diols

HO 20 OH PGAC-C22

HO(CH<sub>2</sub>)<sub>4</sub> — (CH<sub>2</sub>)<sub>4</sub>OH PGAC-C22-DA

presence of a prochiral carbon causes the methylene protons of the ethyl ester group to appear as two distinct quartets. This monomer was first condensed with 1,22-docosane diol<sup>7</sup> under standard trans-esterification conditions at 150 °C using dibutyltin dilaurate as the catalyst to yield PGAC-C22; the polymerization was first done under nitrogen purge, followed by an additional period under reduced pressure to enable formation of higher molecular weight polymer. PGAC-C12 was a highly viscous liquid, whereas the PGAC-C22 was isolated as a white waxy solid. The comparison of the NMR spectra of the monomer and PGAC-C22 clearly reveals the formation of the expected polymer (Figure 1); the explicit disappearance of monomer peaks and formation of new peaks due to the polymer, however, was not clearly evident because of extensive overlap of peaks. For instance, the disappearance of the peaks due to the ethyl ester of monomer, such as the 4.22 ppm peak, is not evident because it is replaced by the methylene ester protons of the polymer; similarly, the methylene proton adjacent to the hydroxyl group in the diol monomer (3.68 ppm) also coincides with the glycol methylene protons in monomer A. The <sup>13</sup>C NMR spectra, however, clearly revealed the complete disappearance of the ethyl ester peaks in the polymer spectra and the appearance of new peaks corresponding to the polyester formation (Figure S1 of the Supporting Information). Whereas both polymers were soluble in organic solvents, like chloroform and THF, they were insoluble in polar solvents, like water and methanol. In water, they formed a lightblue scattering solution suggesting the formation of aggregated particles. Dynamic light scattering studies indicated that the average size of these particles, in case of PGAC-C22, was ~330 nm.8

To examine if these PGACs fold to form the anticipated zigzag structure, we first probed the morphology of the collapsed state using AFM; samples for AFM studies were prepared in two ways — dilute THF solutions (0.05%~w/v) of the polymer were spin-coated onto freshly cleaved mica substrates, and these samples were either solvent-annealed in saturated water vapor or thermally annealed at a temperature

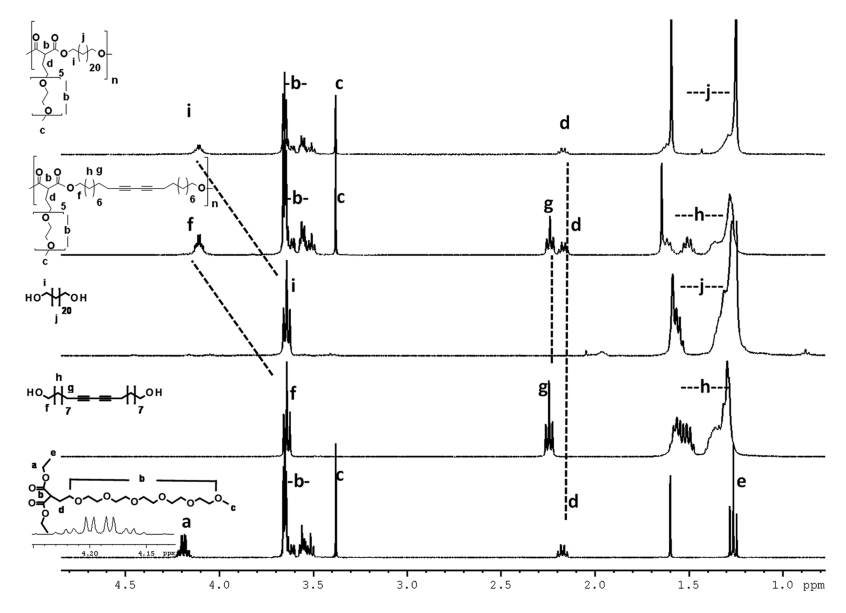
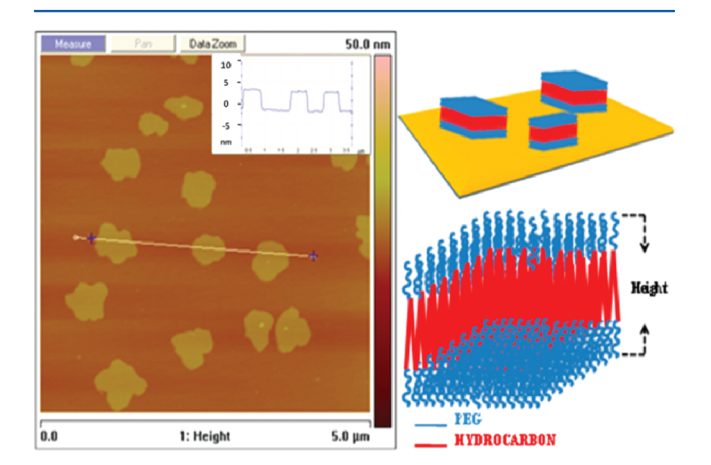


Figure 1. <sup>1</sup>H NMR stack plot of different PGACs along with corresponding monomers.

close to the melting transition ( $\sim$ 60 °C) of the polymer; water vapor is expected to swell the PEG domains and enhance the phase separation. Typically, the aggregate features of thermally annealed samples were more uniform than the solvent-annealed samples. A typical AFM image of the PGAC-C22 is shown in Figure 2.



**Figure 2.** AFM images of PGAC-C22 deposited on mica along with a schematic representation depicting their formation. Inset: line scans depicting the height and lateral dimensions of the flat plate-like aggregates. The coated films were thermally annealed at 60  $^{\circ}$ C for 8 h prior to scanning.

The line scans (Figure 2; inset) reveal the formation of flat plate-like structures with remarkably uniform heights of ~5 nm; the lateral shape and dimensions, however, varied significantly (in the range 350–650 nm). As seen previously in the case of donor—acceptor ionenes, <sup>4</sup> it appears that these structures are formed when the collapsed zigzag chains of the PGACs laterally aggregate to form large plate-like aggregates, as schematically depicted in Figure 2. Similar structures were also seen when the polymers are deposited on Piranha-treated silicon wafers (Figure S2 of the Supporting Information). An estimate of the height of such a folded zigzag structure was obtained by computing the end-to-end distance of a model compound

containing a central C22 alkylene segment flanked by two hexaethylene glycol monomethyl ether units, which was found to be  $\sim$ 6.2 nm. (See the Supporting Information for details.) The slightly lower observed value for the height may reflect the collapsed state of the flexible PEG segments around the relatively rigid alkylene crystallites upon deposition on the hard silicon substrate.

The driving motivation for the formation of these structures arises primarily from two factors: the immiscibility of the alkylene and the HEG segments, which is further reinforced by the strong tendency for the intervening alkylene segments to crystallize in a paraffin-like lattice; the latter effect is known to become dominant when long alkylene segments are present. Therefore, thermal annealing of the sample leads to the effective compaction of the initially formed structures (Figure S2 of the Supporting Information). Although these aggregated structures were formed from THF solutions, the distinctly different solubility parameters of the PEG and the alkylene segments could be expected to lead to their segregation by forming a collapsed zigzag conformation during the evaporation of the THF solvent. In other words, the lower solubility of the alkylene units in THF when compared with the PEG segments would first cause the selective collocation of the alkylene segments as the polymer solution gets concentrated during evaporation; the crystallization of the alkylene segments beyond a certain threshold density could then direct the formation of the proposed collapsed zigzag structures. AFM images of PGAC-C12 (Figure S2 of the Supporting Information) also show similar aggregate structures; however, the aggregates are not perfectly flat and regular. This is clearly due to the fact that at room temperature the C12 alkylene segments are not in a crystalline phase, as will be evident from the DSC studies presented in the following section. AFM studies of light blue aqueous dispersions of PGAC-C22 deposited on mica were also carried out (Figure S2 of the Supporting Information); these images too showed flat plate-like structures with fairly uniform thickness of ~5 nm, thereby confirming that the aggregates formed in water also have similar structures.

To further substantiate our postulate, we carried out DSC studies of both the polymer samples; the PGAC-C22 sample exhibited sharp melting at 61  $^{\circ}$ C, whereas the PGAC-C12

exhibited a melting peak at -8.8 °C (Figure 3), which is consistent with their respective physical states at room

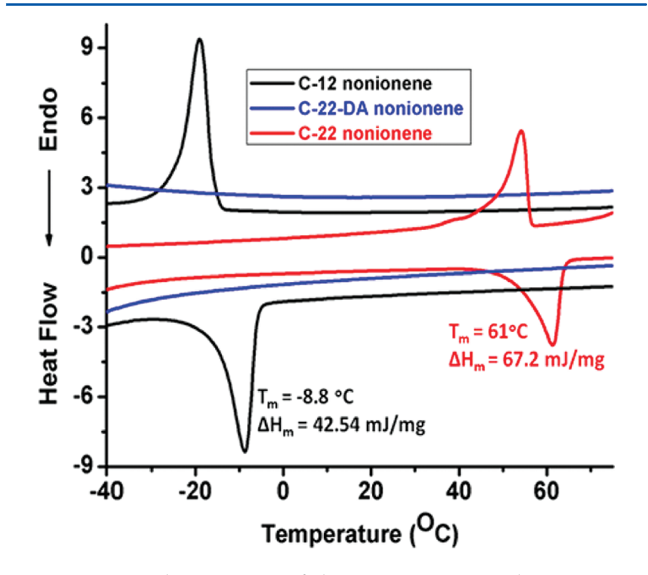
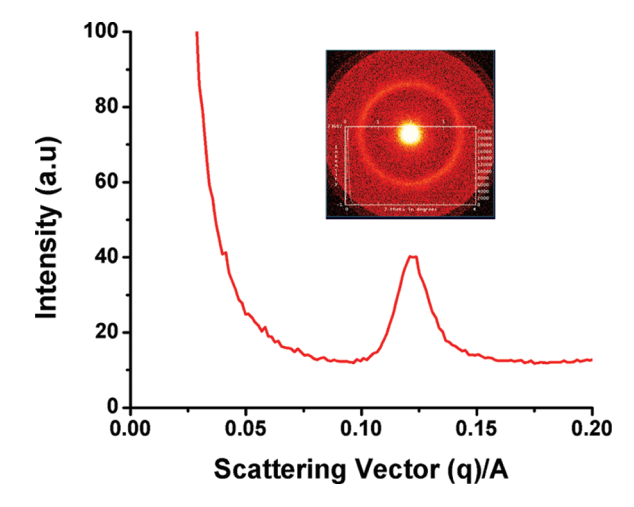


Figure 3. DSC thermograms of the various PGACs; the scans were run at a heating rate of 10 deg/min and are completely reproducible.

temperature. The thermograms were reproducible after the first heating cycle, and the crystallization exotherms were clearly evident during the cooling scans, as seen in the Figure; the enthalpy of melting was significantly higher for PGAC-C22. However, considering the fact that the melting peak is a reflection of the alkylene segments alone, the enthalpies were normalized with respect to the weight-percent of the alkylene segments; the enthalpy values thus obtained were much closer: 150 and 139 mJ/mg for the PGACs, C22, and C12, respectively. These values are roughly in accordance with those seen for *n*-alkane crystals of similar lengths;  $\Delta H_{\rm m}$  for docosane is reported to be 157 mJ/mg. 10 Furthermore, we also carried out DSC studies of the aqueous dispersion (the bluish scattering solution) of PGAC-C22 using a nanocalorimeter; the thermogram (Figure S7 of the Supporting Information) clearly reveals a melting transition at 70 °C with a normalized (with respect to the wt-fraction of alkylene segment) enthalpy of 116 mJ/mg. Although the melting temperature is slightly higher and the enthalpy is lower, it provides a clear indication that the aggregates formed in water may possess a similar paraffinic crystalline lattice, which supports the hypothesis that zigzag collapsed chains formed in water laterally aggregated to form larger bundles.

The tendency for intrachain self-segregation of the alkylene and the PEG segments would also be reflected in the bulk morphology of the sample; small-angle X-ray scattering (SAXS) measurements of PGAC-C22 in the q range: 0.005 to 0.2 Å $^{-1}$  (Figure 4) clearly reveal the formation of an ordered structure. The diffraction pattern exhibits a sharp peak at  $\sim$ 0.1209 Å $^{-1}$  corresponding to a d-spacing of 5.2 nm, which is suggestive of the formation of a layered morphology; observation of the higher order reflections reconfirms the lamellar ordering. This d spacing is clearly in excellent agreement with the average height of the aggregates seen in the AFM images, suggesting that the layered structure may be formed by an assemblage of the smaller aggregated units. In other words, the final structure is the result of assembly of individually folded molecules – making this an interesting case of conformational control at a



**Figure 4.** SAXS profiles of PGAC-C22 (red) at room temperature. Inset depicts the complete 2-D scattering patterns.

single-molecule level leading to a predictable organization in the macroscopic sample. No evidence of such layering is seen in the case of PGAC-C12 at ambient temperature; this confirms that the crystallization of the alkylene segments is essential for the formation of such lamellar morphology. (Recall that the melting temperature of PGAC-C12 is -8.8 °C.) At temperatures below its melting point, SAXS measurements of PGAC-C12 may reveal a peak corresponding to a substantially smaller lamellar spacing. It is well known that branching defects along the polyethylene backbone have a strong influence on the lamellar thickness because of the tendency of these defects to exclude from the paraffinic crystal. <sup>12</sup> In a recent study, Alamo et al. 13 showed that polyethylene containing periodic disruptions due to the presence of a pendant chlorine atom exhibited a similar layered morphology, wherein the crystallite thickness showed a clear dependence on the number of intervening methylene units between adjacent chlorine substituents. The formation of such layered morphology in thin solid films, driven segmental immiscibility, was also seen by Ober and coworkers in ionenes that carried pendant semifluoroalkyl groups.14

To ascertain the structure of the crystallites formed by the alkylene segments, wide-angle X-ray diffraction (WAXD) measurements were performed on the PGAC-C22 sample (Figure 5), which was annealed at a temperature close to its melting point. The WAXD pattern could be readily deconvoluted into three peaks at:  $2\theta = 20.8$  (d = 4.27 Å), 21.7 (d = 4.08 Å), and 22.6° (d = 3.93 Å), in addition to a broad amorphous halo. The d spacings estimated from the diffraction peaks did not match the predicted values for the orthorhombic form but instead reflected the presence of a crystalline arrangement similar to those reported for periodically branched ADMET polyethylenes that possess a branch on every 21st carbon along the polymer backbone. 15 The peaks at  $2\theta = 20.8$  and  $22.6^{\circ}$ , which are identical to the results obtained by Hosoda et al.<sup>16</sup> for the ADMET polyethylenes with ethyl branches, possibly originate from a triclinic lattice; the diffraction peak at  $2\theta = 21.7^{\circ}$  suggests the coexistence of a hexagonal phase. Such a coexistence of more than one phase has been previously observed in precise alkyl branched polyethylenes<sup>15</sup> and also when low levels of chlorine are introduced into the polyethylene backbone. 13 Interestingly, the nascent sample does not exhibit this peak (Figure S3 of the

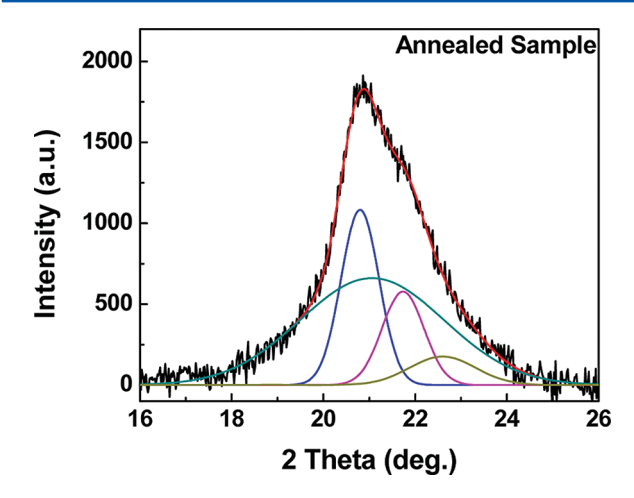


**Figure 5.** WAXS pattern of annealed PGAC-C22 sample, along with the deconvolution showing the presence of three underlying peaks, along with an amorphous halo.

Supporting Information), but it appears on upon annealing, which appears to introduce this additional hexagonal phase. This suggests that the annealing process causes a partial phase transition from triclinic to hexagonal phase, possibly due to differences in the cross-sectional areas of PEG and alkylene segments.

The formation of a zigzag folded structure with hydrophobic alkylene segments in the center and hydrophilic PEG units on either side suggested the possibility that these single folded chains could also organize to form vesicles in aqueous solutions. Hence, we attempted to prepare vesicles of the PGAC-C22 by the standard sonication method; 16 a drop of the vesicular dispersion was put on a carbon-coated grid, and the TEM measurements were carried out. From the TEM images (Figure S5 of the Supporting Information), it was evident that the PGAC-C22 indeed forms fairly large vesicles; sizes ranging from  $\sim$ 100 to 200  $\mu$ m.<sup>17</sup> The presence of biologically benign PEG segments on the outside (and inside) of these vesicular assemblies would be an added advantage for potential applications. In a very recent study, Cho et al. have demonstrated that pendant PEG-grafted hydrocarbon triblock copolymers exhibit anit-fouling properties; 18 this opens up other possible applications of such PGACs.

Finally, in an attempt to transform the collapsed polymer chains into single-chain nanoparticles by an intramolecular cross-linking process, we synthesized another interesting polymer wherein a diol, carrying a diacetylene (DA) unit, was condensed with monomer A. (See Scheme 2.) The resulting polyester, PGAC-C22-DA, had a similar amphiphilic nature that, we reasoned, would enable it to form the folded zigzag conformation in water. However, several attempts to crossstitch the folded structure by photopolymerization of the diacetylene units were unsuccessful, as was evident from the absence of the characteristic absorption peak in the UV-visible spectrum, which is expected from polydiacetylenes.<sup>19</sup> The DSC thermogram of PGAC-C22-DA also revealed that it does not exhibit any melting transition; this suggests that the diacetylene-bearing alkylene segments exhibit a poor tendency to crystallize. This also suggested that the relative disposition of the diacetylene units in the folded polymer was not conducive the topotactic polymerization, which is known to be very sensitive to the interdiacetylene distance and their relative orientation.<sup>20</sup> Evidently the diacetylene units in our collapsed

polymeric structures are unable to adopt the required relative geometry to permit easy transformation to polydiacetylenes. Alternate designs that could enhance the interaction between adjacent alkylene segments in the folded form may be needed, which in turn could permit cross-polymerization of the folded structures.

## CONCLUSIONS

In conclusion, we have developed a simple approach for the preparation of a new class of periodically grafted amphiphilic copolymers (PGAC), wherein hydrophilic pendant HEG units are separated by well-defined hydrophobic alkylene segments. In the case wherein intervening alkylene segment is adequately long, such as 22-carbon chain, the polymer exhibits a strong tendency to adopt a folded zigzag conformation; because of the similarity of this folded structure to those formed by ionenes we suggest a new term, nonionic ionenes (or nonionenes), to describe this class of periodically PEGylated amphiphilic polymers. AFM and SAXS studies of PGAC-C22 suggested the formation of folded zigzag structures; flat pancake-like structures having a thickness of ~5 nm were seen in the AFM images, whereas the SAXS studies revealed the formation of a lamellar morphology with a similar layer-spacing of ~5.2 nm. The motivation to form such zigzag folded structures comes from the intrinsic immiscibility of the alkylene and HEG segments, which is strongly reinforced by the crystallization tendency of long alkylene segments to generate paraffinic-type crystals; the importance of crystallization is also confirmed by the absence of a lamellar morphology in amorphous PGAC-C12. The presence of diacetylene units within the alkylene segment also appears to hinder the generation of the critical length of an all-trans alkylene segment that is essential for the formation of a paraffinic crystal; this in turn precluded the possibility of cross-polymerization of the folded chains, which is an interesting objective that still remains to be achieved. The folded form of the PGAC-C22 may be viewed as a singlemolecule nanoparticle or more appropriately as a PEGylated wax nanobundle because in this case the intervening alkylene segments undergo crystallization to generate a paraffinic-type crystal.<sup>21</sup> Preliminary TEM studies also suggest that large vesicles could also be readily formed from PGAC-C22; the presence of biobenign PEG segments on either side make these assemblies particularly attractive for biological applications. To achieve this, it is essential to impart water solubility to these systems, which should be possible either by increasing the PEG segment length or by developing strategies to place hydroxyl groups at the PEG termini. The simplicity and versatility of the synthetic approach for the preparation this novel class of amphiphilic polymers should open up the possibility of generating several other interesting derivatives that could present some unique application potentials, such as in drug delivery, polar ordering of chromophores, and so on.

## **■ EXPERIMENTAL SECTION**

Materials and Methods. Sodium borohydride, sodium hydride, tosyl chloride, PEG-150, Pd/C (10%), dibutyltin dilaurate (DBTDL), and dodecane diol were purchased from Aldrich Chemical and used as such without further purification. Benzyl chloride, sodium hydroxide, potassium hydroxide, metallic sodium, and tetramethyl ethylene diamine were purchased from Spectrochem Chemical Company and used without further purification. Undecylenic acid was purchased from LEO Chemicals and was distilled before use. All of the solvents were distilled and were dried, if necessary, by the following standard

procedures. 10,11-Dibromoundecanoic acid, 10,11-dibromoundecan-1-ol, undec-10-yn-1-ol, docosa-10,12-diyne-1,22-diol, and docosane 1,22-diol were all synthesized using reported procedures. 22-24 Hexaethylene glycol monomethyl ether monotosylate was synthesized by a previously reported procedure. 25 Structures of all monomers and polymers were confirmed by <sup>1</sup>H NMR spectroscopy and by elemental analysis in the case of the final polymers. NMR spectra were recorded on a Bruker AV400 MHz spectrometer using CDCl<sub>3</sub> as the solvent and TMS as reference. Small-angle X-ray scattering (SAXS) measurements were performed using a Bruker Nanostar, equipped with a rotating anode generator, operating at 45 kV and 100 mA (copper anode,  $\lambda$  = 1.54 Å), three-pinhole collimation, and a 2-D multiwire Histar detector. The SAXS detector was calibrated using silver behenate. The powdered samples were mounted between thin polymer films during measurements. The exposure time for a single frame was, ~7200 s. Two-dimensional SAXS images collected were circularly averaged to 1-D formats (intensity versus q) using the Bruker software; the data are presented after background subtraction. Wide-angle X-ray diffraction (WAXD) measurements were performed on a Bruker AXS D8 advance diffractrometer operating at 40 kV and 30 mA with a scanning rate 1 deg/min, using Cu K<sub> $\alpha$ </sub> radiation ( $\lambda = 1.5406$  Å). Samples were coated within the cavity of the sample holder made of poly(methyl methacrylate). DSC measurements were carried out on a Mettler Toledo instrument at a heating rate of 10 deg/min; the samples were first heated to melt and cooled, and the subsequent heating and cooling runs were recorded. Gel permeation chromatography (GPC) was carried out with a Viscotek TDA model 300 system and is coupled to refractive-index, differential viscometer, and light-scattering detectors in series. The separation was achieved with two mixed-bed PLgel columns (5  $\mu$ m, mixed-bed C) maintained at 35 °C using tetrahydrofuran (THF) as the eluent. The molecular weights were determined using a universal calibration curve based on polystyrene standards. AFM measurements of the polymer samples were performed by using Nanoscope IVA multimode AFM (Digital Instrument, Santa Barbara, CA). All of the images presented are tapping mode height images, recorded using a tip of force constant 2.8 N/m and resonance frequency of 75 kHz. Image analysis was performed using the software provided along with the Nanoscope IVA. Either freshly cleaved mica foil or piranha-treated silicon wafer was used as substrate for the measurements.

Monomer (A). Sodium hydride (0.84 g, 60 wt % in mineral oil, 21.2 mmol) was taken in THF, and the solution was cooled to 0 °C. Diethyl malonate (3.51 g, 26.64 mmol) was added dropwise to the icecold solution, and the reaction mixture was allowed to stir for 2 h at room temperature. To this solution, hexaethylene glycol monomethyl ether monotosylate (4 g, 8.8 mmol) was added, along with catalytic amount of KI, and the reaction mixture was heated to reflux for 12 h. Subsequently, the reaction mixture was cooled to room temperature and THF was removed under reduced pressure; 30 mL water was added, and the entire solution was extracted with ethyl acetate  $(3 \times 50)$ mL). The combined organic layer was concentrated under reduced pressure, and the crude product was purified by distillation in Kugelröhr apparatus at 250 °C and 2 Torr; a viscous colorless liquid was obtained in 65% yield. <sup>1</sup>H NMR ( $\delta$ , CDCl<sub>3</sub>): 1.25 (t, 6H, -COOCH<sub>2</sub>CH<sub>3</sub>); 2.2 (q, 2H, -OCH<sub>2</sub>CH<sub>2</sub>CH-); 3.39 (s, 2H, -OCH<sub>3</sub>); 3.70-3.50 (m, 22H, -OCH<sub>2</sub>CH<sub>2</sub>O-); 3.50 (t, 1H, -CHCOOCH<sub>2</sub>CH<sub>3</sub>); 4.2 (m, 4H, -COOCH<sub>2</sub>CH<sub>3</sub>).

Typical Polymerization. PGAC-C22: 1.0 g (2.28 mmol) of monomer A, along with 0.78 g (2.28 mmol) of docosane-1,22-diol and 2 mol % catalyst (dibutyltin dilaurate), was taken in a test tube-shaped polymerization vessel. The mixture was heated to melt under dry  $N_2$  purge, and the contents were stirred for 15 min to ensure homogenization. Subsequently, the reaction mixture was heated to 150 °C for 2 h under  $N_2$  purging. In the second stage, the polymerization vessel was connected to the Kugelröhr apparatus and the polymerization was continued at 150 °C for an additional 1 h under reduced pressure. The resulting polymer was dissolved in THF and filtered; the filtrate was concentrated under reduced pressure to a viscous solution and precipitated in methanol. The polymers were further purified twice by dissolution in THF and reprecipitated into

methanol to yield a white waxy solid in 83% yield. <sup>1</sup>H NMR (δ, CDCl<sub>3</sub>): 1.25 (m, 36H, -OCOCH<sub>2</sub>CH<sub>2</sub>(CH<sub>2</sub>)<sub>18</sub>CH<sub>2</sub>CH<sub>2</sub>OCO-); 1.6 (m, 4H, -OCOCH<sub>2</sub>CH<sub>2</sub>(CH<sub>2</sub>)<sub>18</sub>CH<sub>2</sub>CH<sub>2</sub>OCO-) 2.18 (q, 2H, -OCH<sub>2</sub>CH<sub>2</sub>CHCOO-); 3.38 (s, 3H, -OCH<sub>3</sub>); 3.70-3.50 (m, 22H, -OCH<sub>2</sub>CH<sub>2</sub>O-); 3.53 (t, 1H, -OCOCHCH<sub>2</sub>CH<sub>3</sub>); 4.12 (m, 4H, -OCOCH<sub>2</sub>CH<sub>2</sub>(CH<sub>2</sub>)<sub>18</sub>CH<sub>2</sub>CH<sub>2</sub>OCO-). Elemental analysis: C, 64.82%; H, 10.96% (Calculated for C<sub>3,8</sub>H<sub>7,2</sub>O: C, 66.3%; H, 10.47%).

The other two polymers, namely, PGAC-C12 and PGAC-C22-DA, were prepared using a similar procedure, details of which are available in Supporting Information.

#### ASSOCIATED CONTENT

## S Supporting Information

Detailed experimental procedures, AFM images of the different polymers, additional X-ray scattering, and DLS data. This material is available free of charge via the Internet at http://pubs.acs.org.

#### AUTHOR INFORMATION

#### **Corresponding Authors**

\*E-mail: raman@ipc.iisc.ernet.in.

#### **Present Address**

<sup>†</sup>Material Sciences and Technology Division, National Institute for Interdisciplinary Science and Technology (NIIST), Thiruvananthapuram – 695 019 Kerala, India

#### Note

The authors declare no competing financial interest.

#### ACKNOWLEDGMENTS

We would like to thank DAE for the ORI award to S.R. and IISc for award of the Centenary Postdoctoral Fellowship to E.B.G.. We thank the Central X-ray facility of IISc and Raman Research Institute for the SAXS measurements and NIIST and Trivandrum for TEM measurements. We would also like to thank Dr V. A. Raghunathan for many valuable discussions regarding the SAXS measurements.

## REFERENCES

- (1) (a) Rembaum, A.; Baumgartner, W.; Eisenberg, A. J. Polym. Sci., Polym. Lett. Ed. 1968, 6, 159–171. (b) Rembaum, A.; Noguchi, N. Macromolecules 1972, 5, 261–269. (c) Noguchi, N.; Rembaum, A. J. Polym. Sci., Polym. Lett. Ed. 1969, 7, 383–394.
- (2) For a recent review on ionenes, see: Williams, S. R.; Long, T. E. *Prog. Polym. Sci.* **2009**, 34, 762–782.
- (3) (a) Kunitake, T.; Nakashima, N.; Takarabe, K.; Nagai, M.; Tsuge, A.; Yanagi, H. *J. Am. Chem. Soc.* **1981**, *103*, 5945–5947. (b) Kunitake, T.; Tsuge, A.; Takarabe, K. *Polym. J. (Tokyo, Jpn.)* **1985**, *17*, 633–640.
- (4) De, S.; Ramakrishnan, S. Macromolecules 2009, 42, 8599–8603.
  (5) (a) Berda, E. B.; Wagener, K. B. Macromol. Chem. Phys. 2008,
- (5) (a) Berda, E. B.; Wagener, K. B. *Macromol. Chem. Phys.* **2008**, 209, 1601–1611. (b) Berda, E. B.; Lande, R. E.; Wagener, K. B. *Macromolecules* **200**7, 40, 8547–8552.
- (6) Yip, K. T.; Zhu, N. Y.; Yang, D. *Org. Lett.* **2009**, *11*, 1911–1914. (7) The C-22 diol was synthesized in three steps using reported procedures from 11,12-undecenol; see the Supporting Information for
- details.
  (8) DLS studies (see Supporting Information) were carried out using a dilute aqueous solution of the C22 PGAC. The estimated size using DLS was slightly lower than the estimate (lateral dimension) from AFM, suggesting that the drying process during spin-casting could
- have led to further aggregation. (9) (a) Carfagna, C.; Roviello, A.; Sirigu, A. *Mol. Cryst. Liq. Cryst.* **1985**, *122*, 151–160. (b) Kaufman, H. S.; Sacher, A.; Alfrey, T.; Frakuchen, I. *J. Am. Chem. Soc.* **1948**, *76*, 3147–3147.

(10) Dirand, M.; Bouraoukba, M.; Briard, A.-J.; Chevallier, V.; Petitjean, D.; Corriou, J.-P. J. Chem. Thermodyn. 2002, 34, 1255–1277. (11) The SAXS data for the PGAC-C22 were also collected in a machine that permitted acquisition over a larger q-range; higher order reflections, confirming the formation of uniformly layered morphology, were clearly visible; see Figure S4 of the Supporting Information. (12) (a) Rees, D. V.; Bassett, D. C. J. Polym. Sci., Part A-2 1971, 9, 385–406. (b) Prime, R. B.; Wunderlich, R. J. Polym. Sci., Part A-2 1969, 7, 2061–2072. (c) Reding, F. P.; Lovell, C. M. J. Polym. Sci. 1956, 21, 157–159. (d) Smith, J. A.; Wagener, K. B. Colloid Polym. Sci. 2004, 282, 773–781. (e) Smith, J. A.; Brzezinska, K. R.; Valenti, D. J.; Wagener, K. B. Macromolecules 2000, 33, 3781–3794. (f) Gutzlerand, F.; Wegner, G. Colloid Polym. Sci. 1980, 258, 776–786. (g) Alamo, R. G.; Mandelkern, L. Macromolecules 1989, 22, 1273–1277.

- (13) Alamo, R. G.; Jean, K.; Smith, R. L.; Boz, E.; Wagener, K. B.; Bockstaller, M. R. *Macromolecules* **2008**, *41*, 7141–7151.
- (14) Wang, J.; Ober, C. K. Macromolecules 1997, 30, 7560-7567.
- (15) (a) Qiu, W.; Sworen, J.; Pyda, M.; Nowak-Pyda, E.; Habenschuss, A.; Wagener, K.; Wunderlich, B. *Macromolecules* **2006**, 39, 204–217. (b) Lieser, G.; Wegner, G.; Smith, J.; Wagener, K. *Colloid Polym. Sci.* **2004**, 282, 773–781. (c) Sworen, J.; Smith, J.; Wagener, K.; Baugh, L.; Rucker, S. *J. Am. Chem. Soc.* **2003**, 125, 2228–2240.
- (16) Hosoda, S.; Nozue, Y.; Kawashima, Y.; Utsumi, S.; Nagamatsu, T.; Wagener, K.; Berda, E.; Rojas, G.; Baughman, T.; Leonard, J. *Macromol. Symp.* **2009**, 282, 50–64.
- (17) For representative TEM pictures of polymeric vesicles formed by block copolymers, see: (a) Discher, B. M.; Won, Y.-Y.; Ege, D. S.; Lee, J. C-M.; Bates, F. S.; Discher, D. E.; Hammer, D. A. *Science* 1999, 284, 1143–1146. (b) Mai, Y.; Eisenberg, A. *J. Am. Chem. Soc.* 2010, 132, 10078–10084.
- (18) Cho, Y.; Sundaram, H. S.; Weinman, C. J.; Paik, M. Y.; Dimitriou, M. D.; Finlay, J. A.; Callow, M. E.; Callow, J. A.; Kramer, E. J.; Ober, C. K. *Macromolecules* **2011**, *44*, 4783–4792.
- (19) (a) Wegner, G. Makromol. Chem. 1972, 154, 35–48. (b) Enkelmann, V.; Wegner, G. Angew. Chem., Int. Ed. Engl. 1977, 16, 416–416. (c) Enkelmann, V.; Leyrer, R. J.; Wegner, G. Makromol. Chem. 1979, 180, 1787–1795.
- (20) (a) Wegner, G. Makromol. Chem. 1971, 145, 85–94. (b) Wegner, G. Z. Z. Naturforsch., B 1969, 24, 824–832. (c) Xu, R.; Gramlich, V.; Frauenrath, H. J. Am. Chem. Soc. 2006, 128, 5541–5547.
- (21) In a recent study, Yin and Hillmyer similarly implicated the crystallization of long alkylene segments in the formation of disk-like micellar aggregates from amphiphilic diblock copolymers. Yin, L.; Hillmyer, M. A. *Macromolecules* **2011**, *44*, 3021–3028.
- (22) Bhanu Prasad, A. S.; Bhaskar Kanth, J. V.; Periasamy, M. Tetrahedron 1992, 48, 4623-4626.
- (23) Narasimhan, S.; Mohan, H.; Madhavan, S. Indian J. Chem., Sect. B: Org. Chem. Incl. Med. Chem. 1995, 34B, 531–534.
- (24) Hay, A. S. J. Org. Chem. 1961, 27, 3320-3321.
- (25) Ramkumar, S. G.; Ramakrishnan, S. *Macromolecules* **2010**, 43, 2307–2312.